Power Electronics and Drives
Volume 4(39), 2019 DOI: 10.2478/pead-2019-0003

sciendo

Power Electronics and Drives

Derivation of Motor Mean Phase Currents in PMSM Drives Operating with Low Switching-to-Fundamental Frequency Ratio

Research Article

Leszek Jarzebowicz

Gdansk University of Technology, Faculty of Electrical and Control Engineering, Narutowicza Str. 11/12, Gdansk, Poland

Received September 27, 2018; Accepted December 27, 2018

Abstract: Pulse width modulation (PWM) of inverter output voltage causes the waveforms of motor phase currents to consist of distinctive ripples. In order to provide suitable feedback for the motor current controllers, the mean value must be extracted from the currents' waveforms in every PWM cycle. A common solution to derive the mean phase currents is to sample their value at the midpoint of a symmetrical PWM cycle. Using an assumption of linear current changes in steady PWM subintervals, this midpoint sample corresponds to the mean current in the PWM cycle. This way no hardware filtering or high-rate current sampling is required. Nevertheless, the assumption of linear current changes has been recently reported as over simplistic in permanent magnet synchronous motor (PMSM) drives operating with low switching-to-fundamental frequency ratio (SFFR). This, in turn, causes substantial errors in the representation of the mean phase currents by the midpoint sample. This paper proposes a solution for deriving mean phase currents in low SFFR PMSM drives, which does not rely on the linear current change assumption. The method is based on sampling the currents at the start point of a PWM cycle and correcting the sampled value using a model-based formula that reproduces the current waveforms. Effectiveness of the method is verified by simulation for an exemplary setup of high-speed PMSM drive. The results show that the proposed method decreases the error of determining the mean phase currents approximately 10 times when compared to the classical midpoint sampling technique.

Keywords: *Electric drives • High-speed drives • Current control • Current measurement • Permanent Magnet Synchronous Drives • Digital Signal Processing*

1. Introduction

1.1. Drives with low switching-to-fundamental frequency ratio

In application fields where size and weight of the electric motor must be minimised, there is a trend of increasing rotor operational speed. For instance, it may be distinctly observed in hybrid and electric cars. For several years, nearly all such cars are equipped with permanent magnet synchronous motors (PMSMs), whose maximum speed exceeds 10000 rpm (El-Refaie et al., 2017). Other examples of applications using high-speed motors are home appliances (Sobczyński, 2016) or turbochargers for combustion engines (Gerada et al., 2014).

Inverter switching frequencies are limited, as they correlate with drive efficiency. Consequently, high-speed operation is associated with a low ratio between inverter switching frequency and fundamental output voltage frequency (shortly: switching-to-fundamental frequency ratio, SFFR). This ratio can drop below the value of 10 (Oleschuk and Barrero, 2014). While new silicon carbide (SiC) transistors allow for increasing the switching frequency (Tarczewski et al., 2018), the rotational speed ranges are also expected to extend further. Hence, the SFFR is not likely to be substantially reduced in the longer time horizon. Moreover, in some cases, six-step control is applied to mitigate the voltage constraint in order to increase the available torque at high speeds (Kwon et al., 2014). In such a case, the SFFR is 6, independently from the dynamic properties of transistors.

* *Email: leszek.jarzebowicz@pg.edu.pl*

1.2. Measurement of motor phase currents

Microprocessor control is featured by distinctive control events repeated in every inverter's pulse width modulation (PWM) cycle (Fig 1).

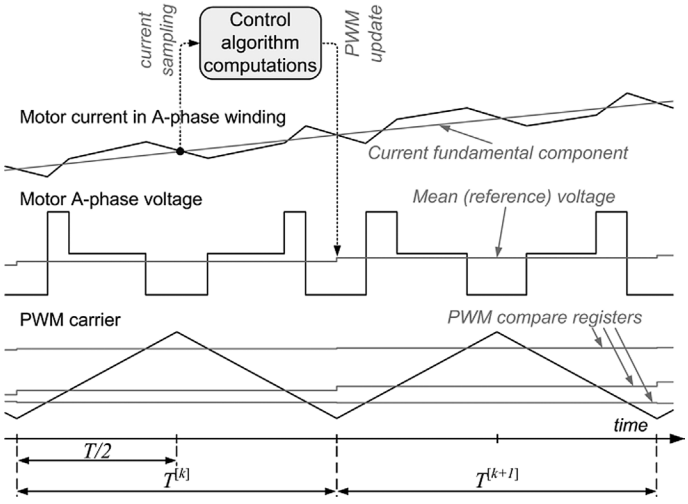

Fig. 1. Timing of the control events in standard control

The control algorithm computations executed in the *k*-th PWM cycle must be completed before the (*k*+1)-th cycle starts, in order to update the reference voltages for this cycle. Furthermore, the computations must be preceded with collecting the control feedback, which includes motor currents. Motor phase currents are represented by complex waveforms related to the modulated voltage. The current ripples depend on the PWM timing, which is set beyond the current control algorithm, and so they are not subject to current control. In turn, the control algorithm aims at regulating the mean currents, and thus such type of value should be provided as a feedback signal. A typical solution to extract the mean current is to sample the current signal at the midpoint of the PWM cycle. Assuming that the voltage waveform is symmetrical and that changes in the current in steady voltage intervals are linear, this midpoint sample represents the mean current in the PWM cycle (Persson, 2002). It is also possible to oversample the current waveform and to compute the mean as the average of samples, but in such a case the result of computation for the *k*-th is available after this cycle ends, and so the control algorithm can use this input to update the reference voltages only in the (*k*+1)-th cycle. This produces an additional control lag that results in the deterioration of dynamic control properties. A similar drawback is introduced if hardware low-pass filtering is applied to extract the mean currents.

1.3. Related research

The methodology of current sampling and processing in microprocessor-controlled electric drives appears to be settled. Nevertheless, some recent research has revealed limitations and introduced new solutions to this field. In the study by Kim et al. (2014), measurement errors introduced by the imperfections of current feedback hardware were studied. The impact of scaling and offset errors in particular phase current sensors on a drive performance was analysed and a suitable error compensation method was proposed. Wolf et al. (2015) indicated that motor phase currents should not be approximated with linear functions when modelling motors featured by short electrical time constants. In this regard, errors of the mean phase current measurement using the midpoint sampling were derived by simulation and experiment. In (Vukosavić et al., 2016) a study on synchronous sampling errors associated with the lockout time, motor cables, winding capacitance and anti-aliasing filters was presented. The authors proposed to suppress these errors by using a period-average filter. Additionally, an amendment to the current controller was advised, in order to partially compensate for the delay caused by low-pass filtering.

Some research on current measurement in electric drives focuses on minimising the hardware cost. Lu et al. (2018) proposed a current reconstruction algorithm that allows for the use of a single current sensor. A model-based compensation scheme was developed to align the samples acquired at shifted instants. Other studies aim at replacing the current sensors by resistors. For instance, in the study by Li and Gao (2018), a case of three resistors installed in series to the

low-side transistors was considered. The authors developed a new sampling method and applied a predictive current model to overcome the problem of short zero-voltage intervals, which arises when the modulation index is high.

Böcker and Buchholz (2013) investigated the impact of current sampling rate on drive control dynamics, proving that oversampling with a ratio of 8 to 16, combined with applying a specific PWM generator, which allows for multiple reference updates within the control intervals, significantly improves the control properties of an electric drive. Nevertheless, typical microprocessors dedicated for electric drive's control allow only for single or double update of the reference voltage in a PWM cycle (Wang et al., 2010).

Some recent researches on current sampling and processing are focused on drives operating with low SFFR. Sepulchre et al. (2016) indicated that current controllers applied in field-oriented control (FOC) rely on the current feedback signals that are adequate for the rotor position corresponding to the instant of current sampling. As the rotor may cover a significant angular distance between current sampling and PWM update, the update should be carried out using a modified angle in inverse Park transformation. The value of this angle is predicted in order to match the midpoint of the next control cycle. Another study (Jarzebowicz, 2017) analyses how operating with low SFFR affects the linear approximation of motor phase currents. The study proves that substantial advancement in the rotor position that takes place in a control cycle makes the phase current waveforms evidently non-linear due to the change in the electromotive force. As a result, the midpoint sample of the phase current does not represent the mean value precisely. The study reports errors of the midpoint sampling technique reaching 4% for a drive operating with an SFFR of 14. Nevertheless, no solution is provided to suppress these errors.

1.4. Problem formulation and paper's aim

Current samples acquired at the midpoint of PWM cycle represent the mean current in the cycle only under an assumption of linear current changes in steady-voltage intervals. As recently reported, this assumption is invalid for low SFFR drives, and the midpoint sampling delivers erroneous feedback in such a case. Consequently, a new approach of deriving mean phase currents is required for low SFFR drives.

This paper proposes a new method for deriving the mean motor phase current, which is robust to low SFFR operation. The approach uses a current sample from the start point of a PWM cycle, and a model-based algorithm that reproduces the mean current. The effectiveness of this method was verified throughout simulations for an exemplary high-speed PMSM drive featured by the minimal SFFR of 15.

2. Proposed solution

The proposed solution changes the timing of control events as shown in Fig 2. The instant of current sampling is shifted to the beginning of the PWM cycle. After the sample is acquired, a mathematical model is used to predict the current waveform within the cycle and to compute the mean current.

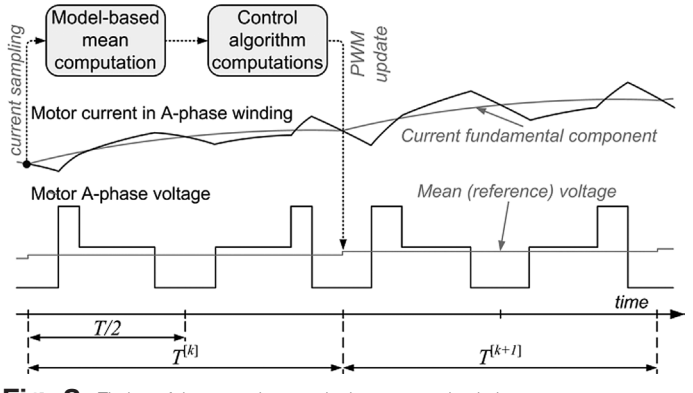

Fig. 2. Timing of the control events in the proposed solution

The PWM in the (k+1)-th control cycle is updated according to the feedback collected in the k-th cycle, and so no additional control lag is introduced to the system. The mathematical model is explained below in the example of processing the A-phase current. Currents in other motor phases are approached in the similar manner.

Using the current value $i_A^{[k]}$ sampled at the start point of the control cycle (at $t = 0$), the waveform of i_A current for a time range $t\epsilon(0, T)$ of the k-th PWM cycle can be modelled as:

$$i_A(t) = i_A^{[k]} + \Delta i_A(t) = i_A^{[k]} + \int_0^t \frac{di_A(t)}{dt} dt \tag{1}$$

The current derivative di_A/dt in Equation (1) is expressed by the following equation:

$$\frac{di_A(t)}{dt} = \frac{u_A(t) - R_s i_A(t) + \psi_f \cdot p\omega(t) \cdot \sin(p\theta(t))}{L_s}, \tag{2}$$

where $u_A(t)$ is the A-phase motor voltage; ψ_f is the permanent magnet flux; p is the number of pole pairs; $\omega(t)$ is the rotor speed; $\theta(t)$ is the rotor position; R_s is the stator winding resistance; and L_s is the stator inductance.

The mean value of the current ripple component, which is related to producing the inverter output voltage by means of modulation, is equal to zero (Persson, 2002). Hence, the model may reproduce only the current fundamental component (shown in Figs 1 and 2), which is a theoretical response to a constant voltage that is equal to the mean of the modulated one in the cycle. As a consequence, the voltage waveform $u_A(t)$ may be reproduced by its mean value $u^{[k]}$.

The waveforms of rotor speed $\omega(t)$ and current $i_A(t)$ are approximated with constants corresponding to samples $\omega^{[k]}$ and $i^{[k]}$ acquired at the start point of the k-th PWM cycle, as only such values are available in a microprocessor-based controller. This simplification is commonly applied to digital models, e.g. in model predictive control (Sandre-Hernandez et al., 2018; Wang et al., 2018). However, in low SFFR drives, the duration of the PWM cycle may constitute a substantial part of the phase current period, and so the current can notably change in the PWM cycle. Nevertheless, the constant current approximation affects only the resistive drop $R_s i_a(t)$, which is small when compared to other terms in the numerator of Equation (2). In some studies on PWM transients, this term is even neglected (Persson, 2002). Hence, even though assuming constant current is considered as a rough approximation, the impact of this assumption on the modelling accuracy is expected to be moderate. In turn, the dynamics of rotor speed is limited by the mechanical moment of inertia, so that assuming the constant speed in the PWM cycle is well justified.

The waveform of rotor position $\theta^{[k]}$ cannot be assumed constant, because the model must reflect the non-linear current changes related to the continuous advancement of the rotor position. Hence, following the constant speed assumption, the position is approximated by a linear function of rotor speed:

$$\theta(t) = \theta^{[k]} + \omega^{[k]} \cdot t \tag{3}$$

The impact of the introduced approximations $\omega(t) = \omega^{[k]}$ and $i_A(t) = i^{[k]}$ on modelling accuracy is approached using simulations, which are described in the following sections.

The approximated formula for modelling the current derivative is finally given as:

$$\frac{di_A(t)}{dt} \cong \frac{u_A^{[k]} - R_s i_A^{[k]} + \psi_f \cdot p\omega^{[k]} \cdot \sin\left(p\theta^{[k]} + p\omega^{[k]} \cdot t\right)}{L_s} \tag{4}$$

By integrating Equation (4) on the interval from 0 to t, the change in current with respect to the start point value $i^{[k]}$ is obtained:

$$\Delta i_A(t) = \int_0^t \frac{di_A(t)}{dt} dt \cong \frac{u_A^{[k]} t - R_s i_A^{[k]} t + \psi_f \cdot \cos\left(p\theta^{[k]}\right) - \psi_f \cdot \cos\left(p\theta^{[k]} + p\omega^{[k]} \cdot t\right)}{L_s} \tag{5}$$

Based on Equations (1) and (5), the mean current $i_{A\_mb}^{[k]}$ can be derived analytically. This, in turn, enables model-based correction of the $i^{[k]}$ sample:

$$i_{\mathrm{A\_mb}}{}^{[k]} = \frac{1}{T}\int_0^T \left(i_{\mathrm{A}}^{[k]} + \Delta i_{\mathrm{A}}(t)\right)dt =$$

$$= i_{\mathrm{A}}^{[k]} + \frac{u_{\mathrm{A}}^{[k]}T}{2L_{\mathrm{s}}} - \frac{R_{\mathrm{s}} i_{\mathrm{A}}^{[k]}T}{2L_{\mathrm{s}}} + \frac{\psi_{\mathrm{f}}\cos\left(p\theta^{[k]}\right)T}{L_{\mathrm{s}}} - \frac{\psi_{\mathrm{f}}\cdot\sin\left(p\theta^{[k]} + p\omega^{[k]}\cdot T\right) - \psi_{\mathrm{f}}\cdot\sin\left(p\theta^{[k]}\right)}{L_{\mathrm{s}}\omega^{[k]}T} \tag{6}$$

3. Simulation model

The model of high-speed PMSM drive represents the discrete control events related to the microprocessor implementation of the control algorithm. The model, whose general structure is shown in Fig 3, was implemented in MATLAB/Simulink. The grey blocks in the figure represent operations, which are executed discretely, once per PWM cycle. Their execution is triggered either by valleys or by peaks of PWM carrier signal (Fig 1), and so it takes place at the start points or midpoints of the control cycle, respectively. Discrete signals are marked with open arrowheads. In contrast, white blocks correspond to subsystems running in the continuous time, and continuous signals are marked with black arrowheads.

The current control algorithm uses the samples corresponding to the midpoints of the PWM cycle. As the computing time is not reflected in the model, the control algorithm is executed infinitely short in the simulation time domain. Thus, it was assumed that the control algorithm is executed at the start points of the control cycle, but it precedes the update of PWM reference signals.

The subsystem representing the PWM modulator uses the space vector PWM (SV-PWM) method (Oleschuk and Barrero, 2014) as shown in Fig 4. Transistors and diodes in the inverter model are assumed ideal. Voltage drops, switching disturbances and dead times are not reflected. The approach to modelling digital control events in MATLAB/Simulink was validated in previous studies (Jarzebowicz, 2017; Jarzebowicz and Mirchevski, 2017) using experimental results.

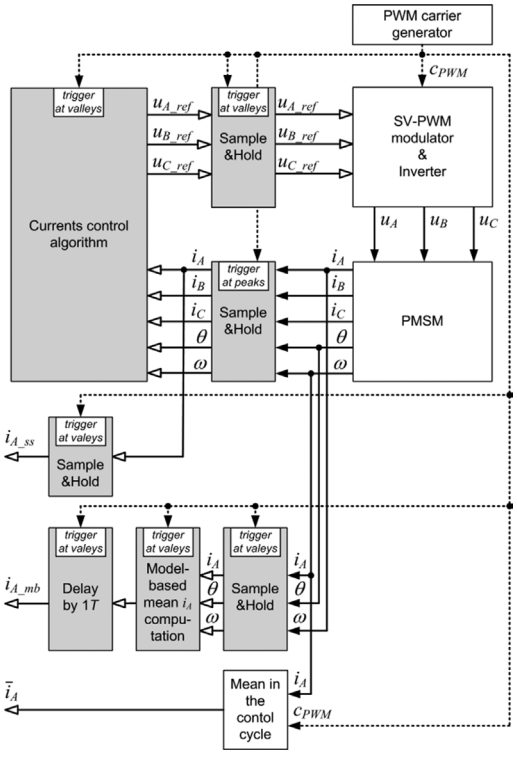

Fig. 3. Structure of the simulation model

Independent from the control algorithm, three discrete values related to the phase current $i_A(t)$ are computed in every PWM cycle. The precise mean current $\bar{i}_A$ is computed by numerical integration of $i_A(t)$ and division of the result by the duration T of PWM cycle. The value of $\bar{i}_A$ is used as a reference for deriving errors of the classical and the proposed method. Another value, marked i_{A_ss}, is obtained by sampling the current synchronously to the midpoints of the control cycle, and so it represents the classical technique. Its update is delayed by a half of the PWM period using the sample and hold block in order to synchronise the updates with the reference signal $\bar{i}_A$. The third value, marked as i_{A_mb}, is derived using the proposed model-based correction algorithm. As the correction uses predicted current waveform, its outcomes are updated one PWM cycle ahead with respect to the reference signal $\bar{i}_A$. Hence, to enable comparison between i_{A_mb} and $\bar{i}_A$ the output signal from the model-based correction signal is delayed by $1T$.

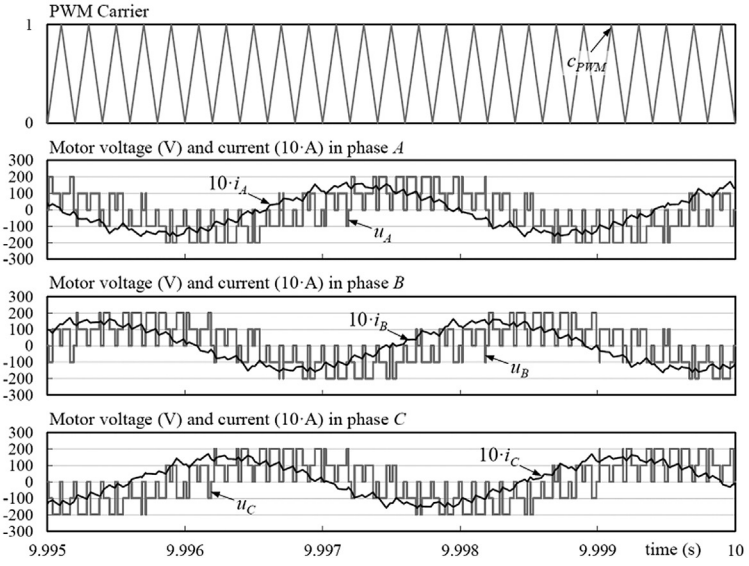

Fig. 4. Exemplary simulation outputs presenting PWM transients (at $p\omega$ = 2100 rad/s)
Abbreviation: PWM, pulse width modulation.

Parameters of the model, given in Table 1, are set up to represent a laboratory high-speed PMSM drive.

Table 1. Parameters of the modelled PMSM drive

Parameters	Value
Control (PWM) frequency $f = 1/T$	5 kHz
Rated phase current I_r	10 A rms
DC-bus voltage U_{DC}	300 V
Rated speed $p\omega_r$	2100 rad/s
Stator resistance R_s	0.1 Ω
Stator inductance $L=L_d=L_q$	1.0 mH
Flux linkage produced by the permanent magnets Ψ_f	75 mWb

Abbreviations: PMSM, permanent magnet synchronous motor; PWM, pulse width modulation.

4. Simulation results

The test scenario consists of accelerating from standstill to the maximum drive's speed. The results are presented in Fig 5. The drive follows the current constraint for the whole test duration, and so rms of the phase current is maintained at the rated value. The fundamental frequency of inverter output voltage reaches 330 Hz at the maximum speed, which for constant switching frequency of 5 kHz corresponds to the SFFR of 15.

The error of deriving the mean phase current by the midpoint sampling distinctively increases with the rotor speed. At the maximal speed, the amplitude of the error waveform exceeds 0.5 A. The error for the proposed method, which is related to the approximations discussed in Section 2, also increases with speed. As speed is associated with the fundamental frequency of inverter output voltage, and this frequency determines the slope rate of current changes, it is presumed that the highest impact on the accuracy is posed by approximating the current waveform $i_A(t)$ by constant $i^{[k]}$. This presumption is confirmed in the last 3 seconds of the test, when the speed is constant, and so the modelling error is related solely to approximating the current by a constant. Generally, the error for the proposed method is kept in a range between −0.05 A and 0.05 A for the whole range of rotor speed. This constitutes 10 times improvement in comparison with the classical midpoint sampling.

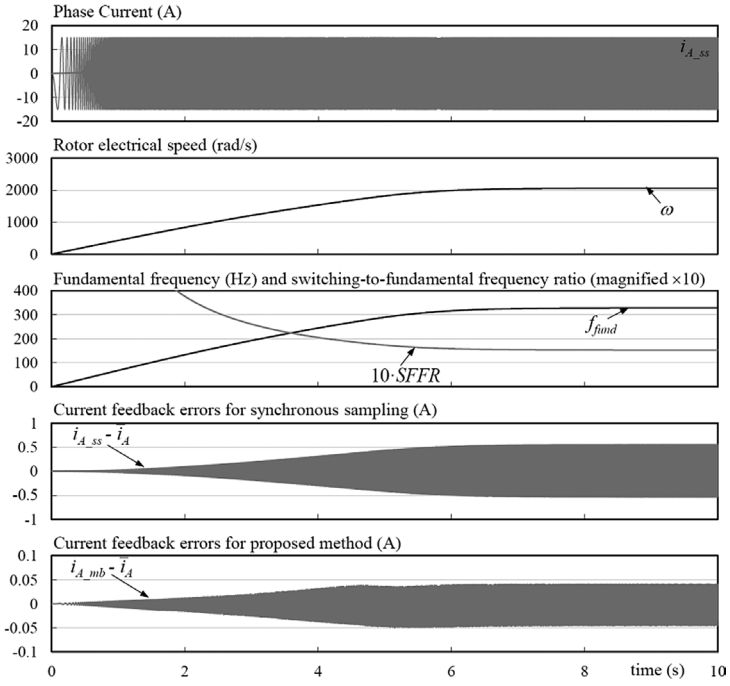

Fig. 5. Simulation results

5. Conclusion

The proposed approach allows for increasing the precision of determining the mean phase currents in low SFFR PMSM drives. The solution does not introduce any extra delay in the timing of discrete control events when compared to the classical midpoint sampling technique. Therefore, the dynamic properties of the drive are sustained, in contrast to other methods such as hardware low-pass filtering or high-rate oversampling.

The simulation study revealed that the errors obtained for the proposed approach increase with rotor speed, similar to the classical midpoint sampling errors. Nevertheless, the errors of the proposed method are 10 times smaller than that of midpoint sampling. In practical implementation, other sources of errors are expected to appear, e.g. motor parameters mismatch, inaccuracy of position and speed measurement. Hence, the accuracy of the proposed method would be application dependent.

As the proposed method shifts the instant of feedback sampling by half of a PWM cycle ahead, and the formula for computing the mean current is relatively simple, there is additional computing time provided for the execution of the control algorithm.

Acknowledgments

This work was supported by the National Science Center, Poland (Grant no. 2018/02/X/ST7/00488).

References

Böcker, J. and Buchholz, O. (2013). Can oversampling improve the dynamics of PWM controls? In: *Proceedings of 2013 IEEE International Conference on Industrial Technology (ICIT)*. Cape Town, 25–28 February 2013, pp. 1818–1824.

El-Refaie, A., Raminosoa, T., Reddy, P., Galioto, S., Pan, D., Grace, K., Alexander, J. and Huh, K. K. (2017). Comparison of Traction Motors that Reduce or Eliminate Rare-Earth Materials. *IET Electrical Systems in Transportation*, 7, pp. 207–214.

Gerada, D., Mebarki, A., Brown, N. L., Gerada, C., Cavagnino, A. and Boglietti, A. (2014). High-Speed Electrical Machines: Technologies, Trends, and Developments. *IEEE Transactions on Industrial Electronics*, 61, pp. 2946-2959.

Jarzebowicz, L. (2017). Errors of a Linear Current Approximation in High-Speed PMSM Drives. *IEEE Transactions on Power Electronics*, 32(11), pp. 8254–8257.

Jarzebowicz, L. and Mirchevski, S. (2017). Modeling the impact of rotor movement on non-linearity of motor currents waveforms in high-speed PMSM drives. In: *Proceedings of 19th European Conference on Power Electronics and Applications (EPE'17 ECCE Europe)*. Warsaw, 11–14 September 2017.

Kim, M., Sul, S.-K. and Lee, J. (2014). Compensation of Current Measurement Error for Current-Controlled PMSM Drives. *IEEE Transactions on Industry Applications*, 50, pp. 3365–3373.

Kwon, Y.-C., Kim, S. and Sul, S.-K. (2014). Six-Step Operation of PMSM with Instantaneous Current Control. *IEEE Transactions on Industry Applications*, 50, pp. 2614–2625.

Li, Z. and Gao, Q. (2018). A Prediction-Based Current Sampling Scheme Using Three Resistors for Induction Motor Drives. *IEEE Transactions on Power Electronics*, 33, pp. 6082–6092.

Lu, J., Hu, Y. and Liu, J. (2018). Analysis and Compensation of Sampling Errors in TPFS IPMSM Drives with Single Current Sensor. *IEEE Transactions on Industrial Electronics*, 66, pp. 3852–3855.

Oleschuk, V. and Barrero, F. (2014). Standard and Non-Standard Approaches for Voltage Synchronization of Drive Inverters with Space-Vector PWM: A Survey. *International Review of Electrical Engineering (IREE)*, 9, pp. 688–707.

Persson, E. (2002). Motor current measurement using time-modulated signals. In: *Proceedings of the Power Conversion Conference*. Osaka, 2–5 April 2002, pp. 716–720.

Sandre-Hernandez, O., Rangel-Magdaleno, J. and Morales-Caporal, R. (2018). A Comparison on Finite-Set Model Predictive Torque Control Schemes for PMSMs. *IEEE Transactions on Power Electronics*, 33, pp. 8838–8847.

Sepulchre, L., Fadel, M. and Pietrzak-David, M. (2016). Improvement of the digital control of a high speed PMSM for vehicle application. In: *Proceedings of 2016 Eleventh International Conference on Ecological Vehicles and Renewable Energies (EVER)*. Monte-Carlo, 6–8 April 2016.

Sobczyński, D. (2016). Review of Solutions Used in High Speed Induction Motor Drives Operating in Household Appliances. *Power Electronics and Drives*, 1(36), pp. 27–49.

Tarczewski, T., Skiwski, M., Grzesiak, L. M. and Zieliński, M. (2018). PMSM Servo-Drive Fed by SIC MOSFETs Based VSI. *Power Electronics and Drives*, 3(38), pp. 35–45.

Vukosavić, S. N., Perić, L. S. and Levi, E. (2016). AC Current Controller with Error-Free Feedback Acquisition System. *IEEE Transactions on Energy Conversion*, 31, pp. 381–391.

Wang, W., Fan, Y., Chen, S. and Zhang, Q. (2018). Finite control set model predictive current control of a five-phase PMSM with virtual voltage vectors and adaptive control set. *CES Transactions on Electrical Machines and Systems*, 2, pp. 136–141.

Wang, H., Yang, M., Niu, L. and Xu, D. (2010). Current-loop bandwidth expansion strategy for permanent magnet synchronous motor drives. In: *Proceedings of the 5th IEEE Conference on Industrial Electronics and Applications (ICIEA)*, Taichung, 15–17 June 2010, pp. 1340–1345.

Wolf, C. M., Degner, M. W. and Briz, F. (2015). Analysis of Current Sampling Errors in PWM VSI Drives. *IEEE Transactions on Industry Applications*, 51, pp. 1551–1560.